Polish J. Chem., **78**, 125–138 (2004)

Resolution of Quenched Fluorescence Mixtures of Two Conformers of *trans*-1-(2-Anthryl)-2-phenylethene by Constrained and Unconstrained Methods of Principal Component Analysis: a Comparative Study

by A.M. Turek[1*], M. Kowalczyk[1] and A. Danel[2]

[1]*Faculty of Chemistry, Jagiellonian University, ul. Ingardena 3, 30-060 Cracow, Poland*
[2]*Department of Chemistry, University of Agriculture, 30-059 Cracow, Poland*

(Received September 15th, 2003)

Two different methods of principal component analysis (PCA) were applied to resolve pure component spectra in the two-component spectral mixture of gradually quenched fluorescence. The two approaches differ by that in the first method one uses an additional physical constraint to arrive at the desired solution, while none of this but simple matrix transformations are used to this aim in the other. Both methods are classified as the approaches of Principal Component Analysis with Self-Modeling (PCA-SM). The first technique is known as PCA-SM-SV, where SV stands for a constraint related to the Stern-Volmer equation, the second method is known as Kubista's approach to two same-sized correlated sets of spectral data matrices. The methods were applied to resolve the pure component fluorescence spectra in the fluorescence mixture of two conformers of *trans*-1-(2-anthryl)-2-phenylethene (*t*-APE) quenched by fumaronitrile in toluene. The results of the application of both methods to precisely measured spectra appear practically equivalent and eventually dispel the controversy existing in the literature about the fluorescence spectral profiles of the *t*-APE$_A$ and *t*-APE$_B$ conformers in favour of the PCA-SM-SV method which results were earlier questioned by the outcome of other methods.

Key words: principal component analysis, curve resolution, correlated spectral data sets, *trans*-1-(2-anthryl)-2-phenylethene fluorescence

Remarkable dependence of the fluorescence spectra of *trans*-1-(2-anthryl)-2-phenylethene (*t*-APE) on the excitation wavelength, λ_{exc}, especially in the long wavelength spectral edge, was long ago suggested by the Fischers as being a manifestation of rotamerism related to two different conformational structures of *t*-APE [1]. It was soon established by the kinetics measurements and differential quenching of the APE fluorescence that the conformer associated with the longer wavelength emission and shorter fluorescence lifetime was the *trans*-APE$_A$ conformer while the other one was the *t*-APE$_B$ conformer [2]. Since that time the "anomalous" fluorescence emission of *t*-APE has been extensively studied by many authors [3–9].

It has been commonly recognized that the equilibrium between almost isoenergetic conformers of *t*-APE ($\Delta H ca.$ 0.3 kcal mol^{-1}) of similar concentration squares very

*Author for correspondence; e-mail: turek@chemia.uj.edu.pl

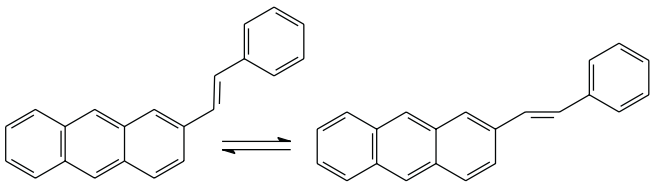

t-APE$_A$ *t*-APE$_B$

well with the Havinga's NEER (NonEquilibration of Excited Rotamers) principle [10], however, the resolution of the fluorescence data matrices of *t*-APE into spectra of pure components raised many questions [5–9]. A typical example of such controversies is a set of the excitation wavelength dependent fluorescence spectra of *t*-APE in toluene. In 1992 Spalletti *et al*. [5] described the resolution of the two-component fluorescence mixture of this system using a PCA-SM method originally developed by Lawton and Sylvestre [11,12]. PCA-SM-LS makes use of unit area normalized experimental spectra. Each such spectrum, in the case of the two-component system, can be represented as a linear combination of two most significant eigenspectra derived by the PCA algorithm from the overall normalized spectral matrix. A pair of the linear combination coefficients, (α_i, β_i), for each *i*-th experimental spectrum, can be easily determined using for instance a concept of a dot product between the spectrum and the corresponding eigenspectra. The pairs of the coefficients characteristic for all normalized experimental spectra line up forming the so called normalization line along which a search is made to find the coefficients of pure component spectra. During the search a strict condition of non-negativity of the intensities of the acceptable pure component spectra is assumed. Thus moving in the opposite directions along the normalization line one can determine the regions where the pure component spectra should be located. Spalletti *et al*. used in their approach an additional criterion of greatest dissimilarity between the spectra belonging to both regions [5]. The pure component spectra of *t*-APE$_A$ and *t*-APE$_B$ derived this way were soon questioned by Saltiel and his coworkers who applied more sophisticated PCA-SM method using an additional physical constraint in the form of the linear Stern-Volmer equation [13]. Introduction of a physical constraint, as opposed to lack of any physical confinements imposed on traditional PCA-SM-LS approach, allows to classify such a method as physically constrained method of factor analysis. The Stern-Volmer equation constraint used in PCA-SM greatly facilitates the derivation of the pure component spectra of *t*-APE [7]. The PCA-SM-SV method requires a spectral matrix in which the excitation wavelength dependent submatrices of spectra contain the fluorescence spectra recorded for the same excitation line and systematically increased amounts of the quencher in successive samples. Due to different fluorescence lifetimes of both *t*-APE conformers the differential quenching of the fluorescence of both species is observed. In this approach the pure component spectra of the *t*-APE fluorescence system are determined in practically independent way de-

spite the fact that the coefficients (α_A, β_A) of the first conformer are related through the corresponding Stern-Volmer equation to the Stern-Volmer constant, $K_{SV,B}$, of the second conformer, and *vice versa* [13]. The pure component fluorescence spectra of the *trans*-APE conformers resolved by Saltiel *et al*. [7] using O_2 as a quencher appeared apparently different, especially in the case of the *t*-APE_B conformer, than the spectra derived by Spalletti *et al*. using the PCA-SM-LS approach [5].

In 1996 Spalletti *et al.* repeated their spectral resolution of the system in question using, in addition to the PCA-SM-LS method, another approach not related to any method of factor analysis [8]. The method known as kinetic fluorescence analysis (KFA) was developed earlier by Birks and coworkers [14]. It is based on the observation of the fluorescence quantum yield and decay kinetics of the conformer mixture as a function of the excitation wavelength. The crucial point in the method is exact determination of so called isoemissive wavelengths in the fluorescence spectral mixture that is the wavelengths at which the total fluorescence intensity is independent of the excitation wavelength. The isoemissive wavelengths can be found either (a) by comparison of the normalized fluorescence spectra observed over the full range of the excitation wavelengths, or (b) by observations of the fluorescence excitation spectra for different values of the emission wavelengths. In the latter case the unit area normalized excitation spectrum measured at the isoemissive wavelength should be indentical to the unit area normalized absorption spectrum. Fluorescence decays measured at the isoemissive wavelengths provide all the information necessary to determine the optimum fractions of the excited molecules belonging to each fluorescing species. These fractions are functions of the excitation wavelength, so at least two excitation wavelengths related to each isoemissive wavelength are required to precisely determine the pure fluorescence spectra of the individual components. The first excitation wavelength corresponds to the maximum fraction of the first species, the second excitation wavelength corresponds to the maximum fraction of the second species. In ideal case all the isoemissive wavelengths should point out to the same optimum excitation lines. The two fluorescence spectra recorded for the two optimum excitation wavelengths are sufficient to decompose the fluorescence mixture into the spectra of individual components. In their paper Bartocci *et al*. claimed to arrive at almost identical results using both PCA-SM-LS and KFA methods so consequently the spectra resolved by the KFA approach were not shown [8]. These findings were once again verified by Saltiel and coworkers who repeated their resolution of the *trans*-APE fluorescence system using the PCA-SM-SV approach applied to degassed samples of *t*-APE in toluene, this time with fumaronitrile as a quencher [9]. While the resolved fluorescence spectrum of *t*-APE_A conformer appears to be almost identical in both papers, the resolved fluorescence spectrum of *t*-APE_B obtained by Saltiel *et al.* [9] differs significantly from the analoguous spectrum derived by Bartocci *et al*. [8]. The PCA-SM-LS and KFA derived flurescence spectrum of *t*-APE_B exhibits much sharper vibronic features as compared to the PCA-SM-SV derived spectrum. Having confirmed their initial spectral assignements [7] Saltiel *et al*. tried to explain why the seemingly independent approaches of PCA-SM-LS and KFA could lead to

identical erroneous spectra. First, convincing arguments against the application of the PCA-SM-LS method as a valid curve resolution method were given. This method suffers mostly from imprecise determination of the valid selective spectral regions that are crucial in resolution of the spectral mixture by this approach. These selective spectral regions are *a priori* unknown and are arbitrarily chosen by the analyst. Sometimes they exist only for one component, as it is for instance in the case of *t*-APE_B fluorescence, but are hidden in the experimental noise for the other. Second, as regards the application of the KFA approach, it requires a very precise determination of the isoemissive points. Saltiel *et al*. recalculated, using the data provided by Bartocci *et al.* [8], the dependence between the composite fluorescence quantum yield and the fraction of the excited molecules belonging to the first species in the APE fluorescence system (this fraction is a function of the excitation wavelength) and found out that this relationship deviates significantly from linearity in a broad range of the excitation wavelengths. Together with their own experimental findings this lead Saltiel *et al.* [9] to the conclusion that the isoemissive point selected by Bartocci *et al*. at 443 nm [8] was incorrect and consequently the whole kinetic fluorescence analysis was called in question.

The above-described controversies concerning the resolution of the pure component spectra of the *t*-APE fluorescence system motivated us to confront the PCA-SM-SV method devised by Saltiel *et al*. [13] with a statistical PCA-SM approach that as we expected could be a more reliable curve resolution procedure than the obsolete PCA-SM-LS approach combined with the kinetic fluorescence analysis [15,16]. Our choice was Kubista's approach to correlated spectral matrices, a method employing Procrustes transformation between closely related two data matrices [17,18].

EXPERIMENTAL

The sample of *trans*-APE was synthesized for the present work by the Siegrist method [19]. Its purity (>99.5%) was checked by HPLC, mass spectrometric and nuclear magnetic resonance analysis.

Fumaronitrile, FMN, (Aldrich) was recrystallized from toluene prior to use as a quencher. Toluene (Aldrich, 99.8%, HPLC grade) as solvent was used without further purification.

All solutions of *trans*-APE in toluene, with and without the added quencher, were degassed by repeated freeze-pump-thaw cycles to about 10^{-5} Torr, after which the ampoules were flame-sealed at a constriction.

The absorption spectra were recorded using a conventional computer-aided UV/VIS spectrophotometer (SPECORD, Carl Zeiss Jena). The fluorescence spectra were measured with a home-made spectrofluorimeter which was equipped with an EMI 955 8B photomultiplier working in single photoncounting mode. All measurements were made at room temperature (*ca*. 22°C).

Theoretical methods: PCA-SM-SV: Assume that *n* unit area normalized experimental spectra are columns of an input matrix Y having *m* rows. A theoretical matrix $\overline{Y}$, which is the best approximation of the input matrix, Y, in the *f*-dimensional space with less random experimental noise, can be represented as a product of an $m \times f$ *scores* matrix $\overline{U}$ and an $n \times f$ *loadings* matrix $\overline{A}$ obtained by the singular value decomposition

$$Y \cong \overline{Y} = \overline{U}\,\overline{\Lambda}\,\overline{V}^T = \overline{U}\,\overline{A}^T \qquad (1)$$

where $\overline{U}$ is an $m \times f$ matrix of eigenspectra (abstract spectra), $\overline{A}^T$ is an $f \times n$ matrix of corresponding combination coefficients, and f is the number of significant factors. Thus, for a two-component system ($f = 2$) each spectrum, y_i, is represented by a point in the two-dimensional eigenvector space, which means that each spectrum is a linear combination of two abstract spectra,

$$y_i = \alpha_i \bar{u}_\alpha + \beta_i \bar{u}_\beta \tag{2}$$

where α_i is the i-th element of the first column of $\overline{A}$ and β_i is the i-th element of the second column of $\overline{A}$. Since the normalization of spectral areas in Y requires that the sum of the elements in y_i should equal unity, the combination coefficients (α_i, β_i) are constrained to fall on the normalization line defined by the eigenvectors $\bar{u}_\alpha$ and $\bar{u}_\beta$ where $\bar{u}_{j\alpha}$ and $\bar{u}_{j\beta}$ are j-th elements in each vector. On the other hand, it is obvious that each normalized experimental spectrum, y_i, can be represented by a linear combination of the spectra of pure components, A and B.

$$y_i = z_{iA} y_A + z_{iB} y_B \tag{3}$$

where z_{iA} and z_{iB} are the corresponding fractional contributions of the pure component spectra, y_A and y_B, of components A and B, respectively. These pure component spectra are also linear combinations of the eigenvectors, and their combination coefficients, (α_A, β_A) and (α_B, β_B), also fall on the normalization line. Summing up all the elements of y_A gives

$$\alpha_A \sum_{j=1}^{f} \bar{u}_{j\alpha} + \beta_B \sum_{j=1}^{f} \bar{u}_{j\beta} = 1 \tag{4}$$

The task of the self-modeling curve resolution is the determination of the pure component combination coefficients. The original method proposed by Lawton and Sylvestre [14,15] for a two-component system and its modified versions are based on two constraints corresponding to two spectral properties. The first requires that the fractional contributions z_{iA} and z_{iB} have to be ≥ 0, and the second requires that y_A and y_B have no negative elements. These two constraints define two regions on the normalization line for acceptable coefficients of the pure component spectra (see Figure 1).

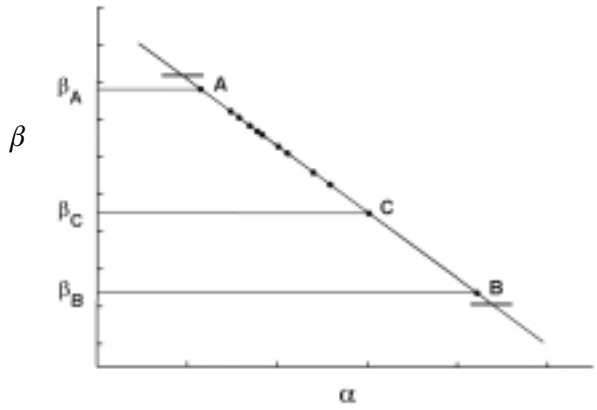

Figure 1. (α – β) normalization line for two-component system including pure component spectra (points A and B). Black bold strokes at both ends of the line define the Lawton-Sylvestre limits for ultimate non-negative spectra. For a two-component spectral mixture (point C) the fractional contribution of the component B, z_B, and hence that of the component A, $z_A = 1 - z_B$, can be calculated according to the lever rule: $z_B = \dfrac{\beta_A - \beta_C}{\beta_A - \beta_B}$.

Unique determination of the coefficients of the pure component spectra requires additional model constraints. Such physical constraints could be for instance: the Stern-Volmer equation constraint [7,9,13] or the van't Hoff equation constraint [20,21]. Since in the present work the latter constraint was not used, only a description of the former approach to PCA-SM is given here.

When one of the experimental variables employed in generating the spectra in Y is the concentration of a quencher, it can be assumed that for an equilibrium mixture of conformers at constant T, the Stern-Volmer constant K_{SV} of each individual conformer is independent of λ_{exc}. This condition provides independent constraints that can aid in the determination of pure component coefficients provided that the K_{SV}'s of individual components are significantly different.

The Stern-Volmer equation for component A is

$$\frac{I_A^0}{I_{iA}} = 1 + (K_{SV})_A[Q_i] \tag{5}$$

where Q_i is the concentration of the quencher in the i-th sample, and I_{iA} is the overall intensity of the fluorescence of the i-th sample, 0 indicates the first sample with no added quencher, $Q_i = 0$. Hence

$$\frac{z_A^0 F^0}{z_{iA} F_i} = 1 + (K_{SV})_A[Q_i] \tag{6}$$

where F^0 and F_i are areas of the fluorescence spectra in the absence and presence of the quencher, prior to normalization, respectively, z_i^0 and z_i are fractional contributions of the A-th component without and with added quencher, and $(K_{SV})_A = k_{qA}\tau_A^0$ is the Stern-Volmer constant of the A-th component where k_{qA} and τ_A^0 are the quenching rate constant and the singlet-state lifetime of the A-th component in the absence of the quencher. For a two-component system the z_A's and consequently the z_B's ($z_B = 1 - z_A$) can be calculated according to the lever rule applied to the ($\alpha - \beta$) normalization line.

$$z_A^0 = \frac{\beta^0 - \beta_B}{\beta_A - \beta_B} \qquad \text{and} \qquad z_A = \frac{\beta_i - \beta_B}{\beta_A - \beta_B} \tag{7 a,b}$$

where β^0 and β_i are coefficients for experimental spectra without and with added quencher, respectively, for a specific λ_{exc}, and β_A and β_B are the coefficients selected for components A and B, respectively. Substitution of (7 a,b) into (6) gives

$$\frac{F^0(\beta^0 - \beta_B)}{F_i(\beta_i - \beta_B)} = 1 + (K_{SV})_A[Q_i] \tag{8}$$

Thus, the Stern-Volmer equation for component A depends only on the combination coefficients of conformer B, and *vice versa*. Minimizing the standard deviation of all points from common Stern-Volmer lines for each conformer yields β_A and β_B. The corresponding α's are obtained using the normalization condition (4).

The difference between the left side and the right side of the Stern-Volmer equation (see 9) upon taking into consideration two (or more) λ_{exc} – series of n samples gives the objective function in nonlinear least squares optimization where a search is performed to find the best fit to the model, *i.e.* K_{SV} and β_B values in a given β_B range.

$$Obj = \sum_{\lambda} \sum_{i=2}^{n} \left(\frac{F_\lambda^0(\beta_\lambda^0 - \beta_B)}{F_{\lambda i}(\beta_{\lambda i} - \beta_B)} - \left\{ 1 + (K_{SV})_A[Q_{\lambda i}] \right\} \right) \tag{9}$$

In (9) λ stands for different λ_{exc}. The best fitting parameters are obtained using 'error function' – STDV which reflects the difference between the left and the right side of the global Stern-Volmer equation (with n samples for various λ_{exc} in each data set) raised to the power of two.

$$\mathrm{STDV} = \frac{1}{2}(Obj)^2 \tag{10}$$

Kubista's approach: In early nineties Kubista and co-workers developed a new method of analyzing correlated spectroscopic data sets [17,18]. It is based on a singular value decomposition of the data and the relation of the sets through Procrustes rotation. Kubista has shown that for two correlated spectral matrices, A and B, of the same dimensions, $m \times n$, the relative concentrations and spectral profiles of the contributing components could be derived without any assumption about the dependence of the concentrations on external factors. The required correlation is that the contributions from the components to the two spectral matrices have the same spectral intensity distributions but different magnitudes of otherwise identical concentration profiles, and the ratio of the magnitudes is a characteristic feature of each component. This condition can be written in matrix notation as

$$\mathrm{A} = \mathrm{SC}^{\mathrm{T}} \tag{11}$$

$$\mathrm{B} = \mathrm{SDC}^{\mathrm{T}} \tag{12}$$

where S is a matrix of real spectral profiles, C is a matrix of real concentration profiles, and D is a diagonal matrix of the scaling elements. The rank of A and B is given by f (if $m \geq n$ then $f \leq n$), the number of components in the mixture.

The matrices A and B have to be decomposed in some orthonormal basis set, using for example singular value decomposition. For both matrices, the orthonormal basis set is the same $\overline{\mathrm{U}}$ matrix, obtained from the decomposition of either the matrix A or the matrix B, or the joint matrix [A B]. The last option is an improvement to Kubista's approach recommended by Booksh and Kowalski [22]. Consequently, we have

$$\mathrm{A} \cong \overline{\mathrm{A}} = \overline{\mathrm{U}}\mathrm{T}_{\mathrm{a}}^{\mathrm{T}} \tag{13}$$

$$\mathrm{B} \cong \overline{\mathrm{B}} = \overline{\mathrm{U}}\mathrm{T}_{\mathrm{b}}^{\mathrm{T}} \tag{14}$$

where $\overline{\mathrm{A}}$ and $\overline{\mathrm{B}}$ are the f-factor SVD reproduced A and B matrices, respectively. Since $\overline{\mathrm{U}}^{\mathrm{T}}\overline{\mathrm{U}} = \mathrm{I}$, where I is an unit matrix with the dimensions $f \times f$, then $\mathrm{T_a}$ and $\mathrm{T_b}$ can be evaluated as

$$\mathrm{T_a} = \overline{\mathrm{A}}^{\mathrm{T}}\overline{\mathrm{U}} \tag{15}$$

$$\mathrm{T_b} = \overline{\mathrm{B}}^{\mathrm{T}}\overline{\mathrm{U}} \tag{16}$$

The matrices $\mathrm{T_a}$ and $\mathrm{T_b}$ have f columns and n rows. They are known from experimental data and the choice of $\overline{\mathrm{U}}$, for example

$$\mathrm{T_a} = \overline{\mathrm{A}}^{\mathrm{T}}\overline{\mathrm{U}} = \mathrm{CS}^{\mathrm{T}}\overline{\mathrm{U}} \tag{17}$$

$$\mathrm{T_b} = \overline{\mathrm{B}}^{\mathrm{T}}\overline{\mathrm{U}} = \mathrm{CDS}^{\mathrm{T}}\overline{\mathrm{U}} \tag{18}$$

By defining

$$\mathrm{W} = \mathrm{S}^{\mathrm{T}}\overline{\mathrm{U}} \tag{19}$$

one obtains

$$\mathrm{T_a} = \mathrm{CW} \tag{20}$$

$$\mathrm{T_b} = \mathrm{CDW} \tag{21}$$

T_a and T_b now contain all information about the objects in matrices A and B. According to Kubista there exists 'Procrustes' rotation of T_a relative T_b, the matrix Q, that minimizes the difference between T_b and T_a Q

$$T_b = T_aQ \tag{22}$$

The matrix Q has dimensions $f \times f$. It has full rank and can be determined by the least squares method

$$Q = (T_a^T T_a)^{-1} T_a^T T_b \tag{23}$$

Combining (20), (21) and (22) allows to write

$$CDW = CWQ \tag{24}$$

where C is a standing rectangular matrix with n rows and f columns. A pseudo-inverse of C has now to be found with the property $C^+C = I$ where I has dimensions $f \times f$. If the rank of C is f then such a matrix does exist [17,18]. This gives important relation

$$WQ = DW \tag{25}$$

All these matrices have dimensions $f \times f$ and D is diagonal. By transposing both sides of (25) one gets an ordinary nonsymmetric eigenvalue equation

$$Q^TW^T = W^TD \tag{26}$$

The concentrations of the components are obtained as the column vectors of the matrix C calculated from (20).

$$C = T_aW^{-1} \tag{27}$$

The pure spectral profiles of the components are now determined upon simple transformation of (19)

$$S^T\overline{U} = W\overline{U}^T\overline{U} \quad (28) \qquad S^T = W\overline{U}^T \quad (29) \qquad S = \overline{U}W^T \quad (30)$$

The diagonal elements (eigenvalues) of the matrix D have their correct values but the concentrations and spectral profiles must be normalized. The normalization is arbitrary and one can choose among few alternative ways [18].

RESULTS AND DISCUSSION

PCA-SM-SV method does not imply any limitations for a number of spectral matrices measured for different excitation lines that can be simultaneously processed. Such limitation is, however, intrinsic in the approach proposed by Kubista in which only two matrices are processed. Consequently, in order to precisely compare the results of both algorithms, the two exactly the same spectral matrices should be taken.

The main task of this work was the resolution of the fluorescence spectra of two rotamers of *t*-APE and comparison of the results with those previously obtained by Bartocci *et al*. [8] and Saltiel *et al*. [9]. Because the fluorimeter Hg lamp, used as a source of light, provided only some discrete excitation lines, the 'suitable' excitation lines were set at 365 and 405 nm, respectively (see Figure 2). It was assumed that the differences in the absorbance for the two components at these lines were sufficient to obtain Kubista's *d*-related matrices of fluorescence,

$$d_{11} = k\,\frac{Abs_{t-APE_A(\lambda_{405})}}{Abs_{t-APE_A(\lambda_{365})}} \qquad \text{and} \qquad d_{22} = k\,\frac{Abs_{t-APE_B(\lambda_{405})}}{Abs_{t-APE_B(\lambda_{365})}} \qquad (31\ \text{a,b})$$

where k is the relative intensity of the applied Hg excitation lines. Consequently, the two matrices of quenched fluorescence, A and B, were measured for the two excitation lines, 365 and 405 nm, respectively.

Selective quenching of fluorescence of the *t*-APE conformers was achieved by using fumaronitrile as a quencher, Q ([Q] = 0.0, 0.0167, 0.034, 0.0050, and 0.00667 M). The spectra were recorded in triplets, baseline corrected and next averaged. Each averaged single spectrum has been interpolated into 0.5 nm intervals and smoothed one time. The spikes of the scattered light observed in all measured spectra and centered at 365 nm (matrix A) and 405 nm (matrix B) were removed. The procedure which enables to do so goes on as follows: First two abstract spectra obtained from SVD for

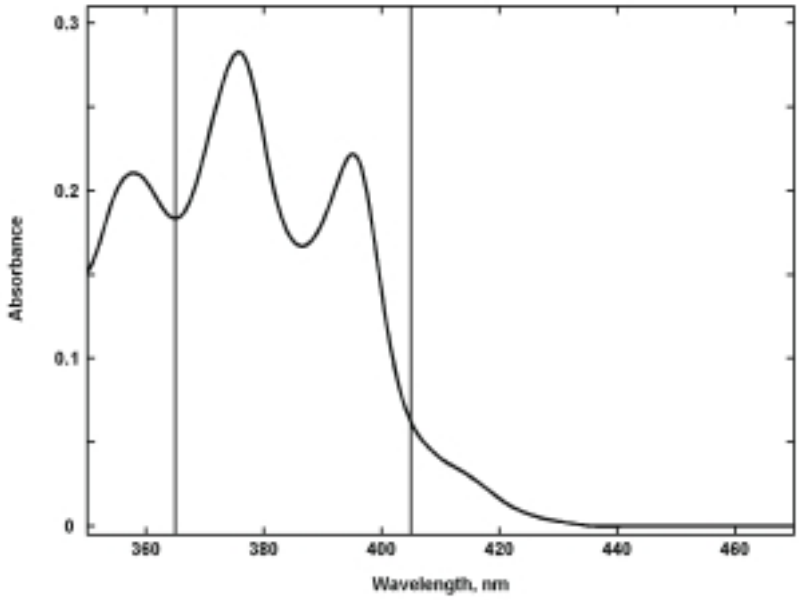

Figure 2. Absorption spectrum of *t*-APE in toluene ($c_{t\text{-APE}} = 1.56 \times 10^{-5}$ M) with vertical lines marking the excitation wavelengths at 365 and 405 nm, respectively.

the matrix B are used as a linear combination to restore a spectral region void of the spike contributions in the spectra belonging to the matrix A. The reverse approach is used to extract the spikes in the matrix B. Removal of the spikes performed in this way leads to exactly two-component spectral system in both data matrices A and B. Multiplication of the spectra by the photomultiplier sensitivity function makes both matrices corrected for nonlinearities of instrumental response. In the pretreatment of the data matrices, A and B, the correction for self-absorption is also applied.

In Figure 3 the fluorescence spectra of *t*-APE belonging to the two excitation lines, 365 and 405 nm, respectively, are shown. The five high intensity emission spectra measured for the excitation wavelength of 365 nm are included in the matrix A, the five low intensity emission spectra recorded for the excitation wavelength of 405 nm form the matrix B. Analysis of the joint matrix [A B] reveals that first two factors account for most of the variance of the matrix (99.7%). The corresponding abstract spectra are shown in the inset to Figure 4. This figure shows the (α,β) normalization line for the *t*-APE fluorescence system with the spectra clustered in two groups belonging either to the matrix A or to the matrix B (only first representatives of these spectral data sets with no added quencher are clearly marked in Figure 4 as a0 and b0, respectively).

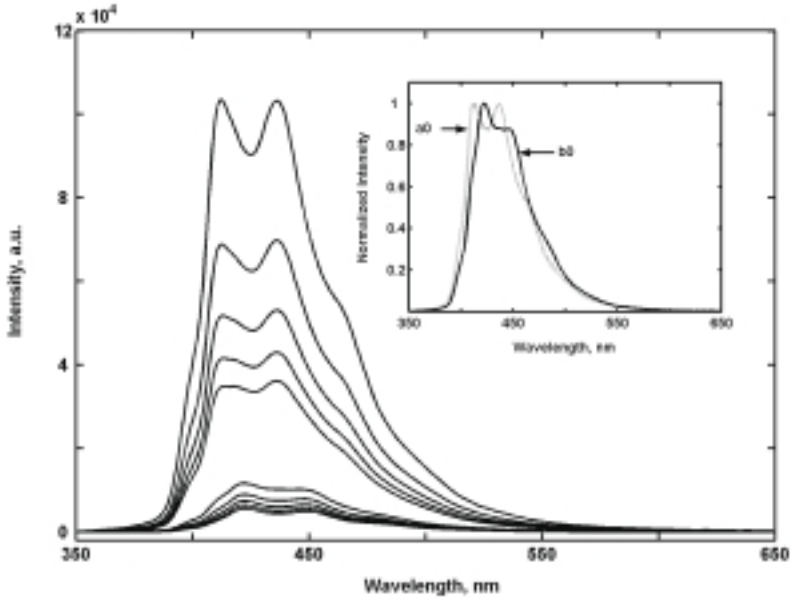

Figure 3. Fluorescence spectra of *t*-APE in toluene ($c_{t\text{-APE}} = 4.95 \times 10^{-5}$ M). Matrix A consists of five high intensity spectra (excitation line at 365 nm), matrix B includes five low intensity spectra (excitation line in the onset of the *t*-APE absorption spectrum at 405 nm). In the inset the normalized spectra of first representatives of each set are shown (samples without quencher).

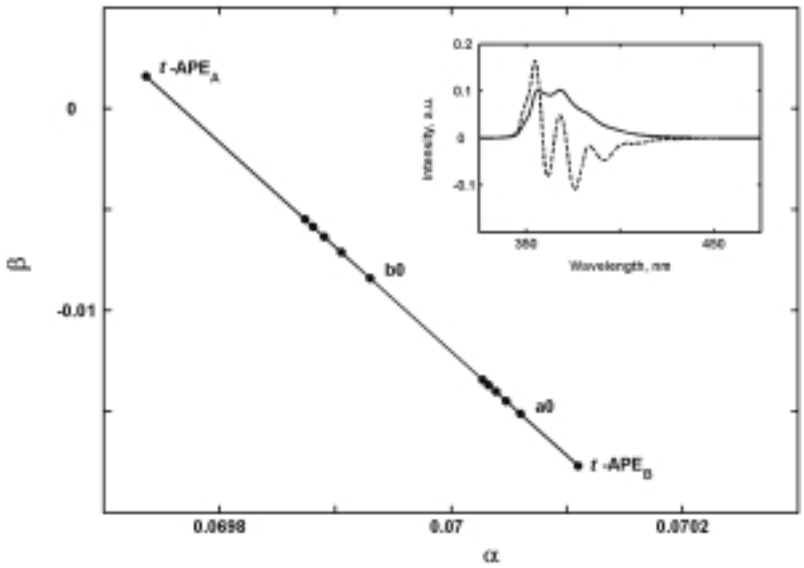

Figure 4. (α,β) normalization line for the joint matrix [A B] of quenched fluorescence mixture of *t*-APE conformers. In the inset the first two significant eigenspectra obtained by SVD for the joint matrix are shown.

In Figure 5 the resolved fluorescence spectra of *t*-APE$_A$ and *t*-APE$_B$ conformers are displayed. Both applied approaches of PCA-SM, *i.e*. PCA-SM-SV and Kubista's methods, produce eventually almost identical spectra of single species, however, some subtle differences can still be observed. It turns out that by its very nature the PCA-SM-SV method is sensitive to the correct amounts of the quencher concentrations entered as a vector to the least square optimization procedure that makes use of the objective function formulated by means of the Stern-Volmer equation. If the true concentrations of the quencher in the samples are sligthly different than the intended ones then the derived pure component spectra may be slightly deformed. In the case of the *t*-APE system it does affect the shape of the resolved *t*-APE$_A$ fluorescence spectrum, and practically does not affect the spectral profile of the resolved *t*-APE$_B$ fluorescence spectrum (for comparison see [7]). The application of the Kubista's method to the data matrices, A and B, produces slightly different fluorescence spectrum of the *t*-APE$_A$ conformer. In fact, it yields even two such spectra. The reason for that lies in the method itself. The Procrustes transformation may be done in two ways: either A → B or B → A. Though the Kubista's approach does not care about the correct values of the quencher concentrations, yet it is very sensitive to the proper shape of the abstract concentration (or more precisely intensity) profiles. As it can be inferred from Figure 4 the fractional contributions of both pure component spectra are more even in the case of the data matrix B (405 nm ecitation line) than in the case of the data matrix A (365 nm excitation line). In the latter case the *t*-APE$_B$ component dominates in the fluorescence mixtures. Consequently, the *t*-APE$_A$ conformer possesses poorer representation in the matrix A, and thus in the abstract concentration profiles obtain-

ed for this matrix. Therefore, small experimental errors reflected in the shape of the spectra collected in A are more significant for the A → B route than similar small experimental errors reflected in the shape of the spectra collected in B for the B → A route. These differences are demonstrated in the inset to Figure 5. The onset of the *t*-APE_A fluorescence spectrum derived by the Kubista's approach for the A → B route (dashed line) deviates more from the onset of the PCA-SM-SV derived *t*-APE_A spectrum than the onset of this spectrum derived by the same method for the B → A route (dash-dotted line). The latter is almost coincident with the PCA-SM-SV pattern. The resolved pure fluorescence spectrum of the *t*-APE_B conformer does not exhibit a similar dependence. The pure component fluorescence spectra of the *t*-APE spectral mixture resolved by the Kubista's approach (the B → A route) and those obtained by the PCA-SM-SV method are almost identical (see Figure 5).

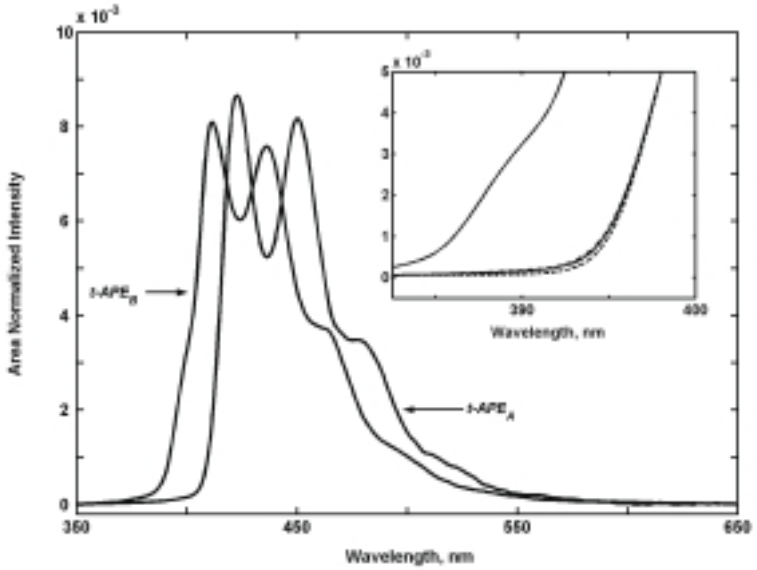

Figure 5. Pure fluorescence spectra of *t*-APE conformers resolved by PCA-SM-SV and Kubista's (B → A) methods. In the inset the leading edges of the spectra derived by PCM-SM-SV approach (solid line) and on Kubista's A → B (dashed line) and B → A (dash-dotted line) routes are shown.

Including pure component spectra to the (α, β) normalization line determined by the spectra of the two-component mixtures allows evaluating the spectral contributions of both quenched fluorescing species in all the two-component spectra by means of the lever rule. This in turn allows to make the corresponding Stern-Volmer plots (see Figure 6). Since there are two spectral matrices, A and B, thus for each species an averaged quenching intensity profile can be calculated. The final averaged Stern-Volmer constants obtained for the quenched fluorescence of *t*-APE_A and *t*-APE_B are 100.29 and 313.47 M^{-1}, respectively, values close to those obtained by Saltiel *et al*. for the same system at 19.3°C (115.5 and 328.7 M^{-1}, respectively) [9].

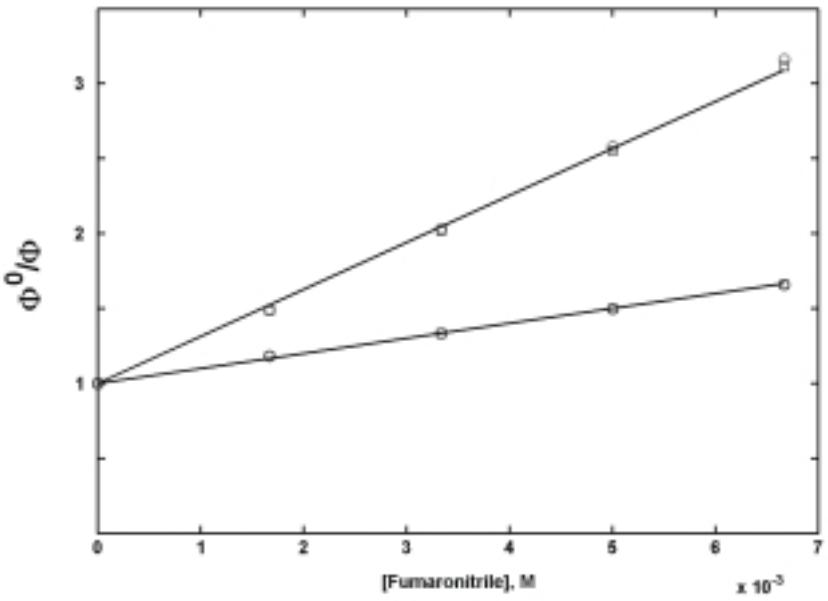

Figure 6. Global Stern-Volmer plots for fumaronitrile quenching of resolved *t*-APE_A and *t*-APE_B fluorescence in toluene. Open squares are related to the intensity quenching profiles obtained by PCA-SM-SV and open circles are related to the averaged intensity quenching profiles obtained by Kubista's approach. Straight lines correspond to the averaged results provided by both methods.

Our fractional contributions of the APE_A fluorescence (z_{APE_A}) to the unquenched fluorescence spectra of *t*-APE, equal 0.13 for λ_{exc} = 365 nm and 0.48 for λ_{exc} = 405 nm, respectively, can be compared with those predicted by Bartocci *et al*. [8]. Using Eq. (3) proposed by Birks *et al*. [14], and taking after Saltiel *et al*. [9] the fluorescence quantum yields of both conformers as $\Phi_A = 1.0$ and $\Phi_B = 0.88$, respectively, and retrieving from Bartocci *et al*. [8] the absorption fractions f_A(365 nm) = 0.115 and f_A(405 nm) = 0.300 one can arrive at $z_{APE_A} = 0.13$ for λ_{exc} = 365 nm and $z_{APE_A} = 0.33$ for λ_{exc} = 405 nm, respectively. Thus, the latter value retrieved in this way from [8] seems to be evidently underestimated.

CONCLUSIONS

Model-based approaches, applying physical constraints and classical nonconstraint chemometric techniques of curve resolution, are two types of methods of PCA-SM to extract the spectra of individual components from matrices of spectral mixtures. By a suitably designing the experiment, it is possible to take simultaneously advantage of both ways of spectral resolution. Both such approaches, one belonging to the group of the constrained methods (PCA-SM-SV) and another one adherent to the class of the unconstrained methods (Kubista's algorithm), have been used in the present work to elucidate the controversial problem of spectral resolution of the *trans*-1-(2-anthryl)-2-phenylethene fluorescence mixture into the contributions from

individual constituents (*t*-APE conformers). An almost excellent agreement between the results of both procedures testifies in favour of the formerly questioned PCA-SM-SV method of curve resolution devised by Saltiel *et al*. [13]*.

Acknowledgments

A. M. T. wishes to thank Professor Jack Saltiel for encouragement and stimulating discussion during preparation of the present paper. A. D. gratefully acknowledges the financial support from the Polish State Committee for Scientific Research, grant No. T11B07518.

REFERENCES

1. Fischer G. and Fischer E., *J. Phys. Chem*., **85**, 2611 (1981).
2. Wismontski-Knittel T., Das P.K. and Fischer E., *J. Phys. Chem.*, **88**, 1163 (1984).
3. Ghiggino K.P., Skilton P.F. and Fischer E., *J. Am. Chem. Soc*., **108**, 1146 (1986).
4. Bartocci G., Masetti F., Mazzucato U., Baraldi I. and Fischer E., *J. Mol. Struct*., **193**, 173 (1989).
5. Spalletti A., Bartocci G., Masetti F., Mazzucato U. and Cruciani G., *Chem. Phys*., **160**, 131 (1992).
6. Karatsu T., Yoshikawa N., Kitamura A. and Tokumaru K., *Chem. Lett*., 381 (1994).
7. Saltiel J., Zhang Y., Sears D.F. Jr. and Choi J.-O., *Res. Chem. Intermed*., **21**, 899 (1995).
8. Bartocci G., Mazzucato U. and Spaletti A., *Chem. Phys*., **202**, 367 (1996).
9. Saltiel J., Zhang Y. and Sears D.F. Jr., *J. Phys. Chem. A*, **101**, 7053 (1997).
10. Jacobs H.J.C. and Havinga E., *Adv. Photochem*., **11**, 305 (1979).
11. Lawton W.H. and Sylvestre E.A., *Technometrics*, **13**, 617 (1971).
12. Sylvestre E.A., Lawton W.H. and Maggio M.S., *Technometrics*, **16**, 353 (1974).
13. Saltiel J., Sears D.F. Jr., Choi J.-O., Sun Y.-P. and Eaker D.W., *J. Phys. Chem. A*, **98**, 35 (1994).
14. Birks J.B., Bartocci G., Aloisi G.G., Dellonte S. and Barigelletti F., *Chem. Phys*., **51**, 113 (1980).
15. Cruciani G., Spalletti A. and Bartocci G., *Z. Phys. Chem*., **172**, 227 (1991).
16. Bartocci G., Spalletti A., Masetti F. and Cruciani G., *J. Mol. Struct*., **165**, 165 (1993).
17. Kubista M., *Chemom. Intell. Lab. Syst*., **7**, 273 (1990).
18. Scarminio I. and Kubista M., *Anal. Chem*., **65**, 409 (1993).
19. Siegrist A.E., Liechti P., Meyer H.R. and Weber K., *Helv. Chim. Acta*, **52**, 2521 (1969).
20. Sun Y.-P., Sears D.F. Jr. and Saltiel J., *J. Am. Chem. Soc*., **110**, 6277 (1988).
21. Saltiel J., Sears D.F. Jr. and Turek A.M., *J. Phys. Chem. A*, **105**, 7569 (2001).
22. Booksh K.S. and Kowalski B.R., *J. Chemometrics*, **8**, 287 (1994).
23. Sanchez E. and Kowalski B.R., *Anal. Chem*., **58**, 496 (1986).
24. Sanchez E. and Kowalski B.R., *J. Chemometrics*, **2**, 247 (1988).

*On the margin, it should be noticed that the applied Kubista's approach is not the only one that could be confronted with PCA-SM-SV. The very nature of the correlated data matrices processed in this work allows to reach for other chemometric methods of curve resolution, for instance the generalized rank annihilation method (GRAM) of Sanchez and Kowalski [23,24]. This method has been shown to be a generalization of Kubista's approach and to overcome many problems associated with the Kubista algorithm. Yet it should be stressed here that when the criteria of applicability of Kubista's approach are strictly met, then the results of both approaches are practically identical (the results of GRAM are unshown in this work for the sake of clarity of presentation).